IAEA nuclear fusion

PAPER • OPEN ACCESS

Suppression of runaway electrons by mode locking during disruptions on J-TEXT

To cite this article: Z.Y. Chen *et al* 2018 *Nucl. Fusion* **58** 082002

OPEN ACCESS
IOP Publishing | International Atomic Energy Agency

Nuclear Fusion

Nucl. Fusion **58** (2018) 082002 (7pp)

https://doi.org/10.1088/1741-4326/aab2fc

Suppression of runaway electrons by mode locking during disruptions on J-TEXT

Z.Y. Chen[1,2], Z.F. Lin[1], D.W. Huang[1], R.H. Tong[1], Q.M. Hu[1], Y.N. Wei[1], W. Yan[1], A.J. Dai[1], X.Q. Zhang[1], B. Rao[1], Z.J. Yang[1], L. Gao[1], Y.B. Dong[3], L. Zeng[4], Y.H. Ding[1], Z.J. Wang[1], M. Zhang[1], G. Zhuang[1], Y. Liang[1], Y. Pan[1], Z.H. Jiang[1] and J-TEXT Team[1]

[1] International Joint Research Laboratory of Magnetic Confinement Fusion and Plasma Physics, State Key Laboratory of Advanced Electromagnetic Engineering and Technology, School of Electrical and Electronic Engineering, Huazhong University of Science and Technology, Wuhan, 430074, China

[2] Chengdu University, Chengdu 610106, China

[3] Southwestern Institute of Physics, PO Box 432, Chengdu 610041, China

[4] Institute of Plasma Physics, Chinese Academy of Sciences, Hefei 230031, China

E-mail: zhhjiang@hust.edu.cn

Received 23 November 2017, revised 14 February 2018
Accepted for publication 28 February 2018
Published 22 June 2018

Abstract

The generation of runaway electrons during disruptions poses a serious threat for the operation of ITER. The efficiency of the injection of large amounts of impurities by massive gas injection or shattered pellet injection to achieve runaway suppression might be compromised due to low gas mixture efficiency and the high Rosenbluth density for runaway suppression. The transport of runaway electrons is dominated by magnetic perturbations. The magnetic perturbations have the advantage of expelling the runaway seeds before they reach high energy. Robust runaway suppression has been reached on J-TEXT with mode locking by the application of $m/n = 2/1$ resonant magnetic perturbations before the thermal quench. The mode locking implemented large magnetic islands inside the plasma which acted as an explosive bomb during disruptions and led to stronger stochasticity in the whole plasma cross section. The NIMROD simulation indicates that this strong stochasticity expels the runaway seeds and results in runaway free disruptions on J-TEXT. This might provide an alternative runaway suppression technique during disruptions for large-scale tokamaks.

Keywords: runaway electron, disruption, mode locking, magnetic perturbation

(Some figures may appear in colour only in the online journal)

1. Introduction

Disruptions in ITER are prone to generate a large fraction of runaway current. About 70% plasma current could be converted into runaway current during disruptions on ITER. The magnitude of the damaging effects due to runaway electrons (REs) increases with the plasma current [1–5]. The prevention and mitigation of disruptions are critical issues for advancing the tokamak concept as a viable fusion energy source. Both the heat loads and the electromagnetic force have been mitigated with a moderate amount of impurities [4] by massive gas injection (MGI) or shattered pellet injection (SPI). It is generally thought that the heat load and halo current reduction capabilities of MGI shutdown will scale well to ITER.

Avoidance and mitigation of the damage due to disruption generated runaway electrons is high priority task for reliable operation of ITER [6]. There are, generally, three mechanisms for RE generation: Dreicer generation, secondary generation (avalanche generation), and hot tail generation [7–9]. The seed electrons from tritium decay also act as runaway seeds in ITER D-T operation phase. The Compton scattering of gamma rays emitted by the activated wall will contribute to the runaway generation also. In a disruption, the Dreicer, tritium decay, the Compton scattering seed and the hot tail processes can create a runaway seed population which will be amplified by the secondary avalanche mechanism. The hot tail process can contribute the runaway generation significantly in fast shutdown experiments [10–13]. A severe consequence of a disruption on ITER could be the generation of a 10 MA RE beam with energies of several tens of MeV that could damage the vacuum vessel and the structures of the machine if it hits the wall without mitigation [8]. Many experiments have been pursued toward understanding the physics of RE generation and suppression during disruptions [14–22]. During the termination phase of the disruption, the conversion of magnetic energy of the runaway plasma into runaway beam kinetic energy can increase substantially the energy deposited on the first wall by the runaway electrons. The conversion of magnetic energy into runaway kinetic energy during termination has been observed on JET, DIII-D and FTU [4–6]. The runaway kinetic energy gain for the conversion of magnetic energy into runaway kinetic energy during the termination phase of the disruption in ITER can be one order of magnitude (up to hundreds of MJs) larger than the plateau runaway kinetic energy [23]. The mitigation of runaway damage during disruption in ITER 15 MA operation is therefore essential.

There are two strategies for preventing the conversion of the plasma current into runaway current during disruptions: (1) Increasing the electron density significantly by massive injection of noble impurities [4, 9, 24, 25]. The densification of the electron density can prevent the formation of runaway current by enhancing the drag force from the background drag to overcome the force from the parallel electric field. (2) Enhancing the magnetic perturbation to the level of destroying confining magnetic surfaces and decoupling the confinement of runaway electron seeds [18, 21, 24, 26]. If all the magnetic surfaces for the confinement of runaway electrons are destroyed for a sufficiently long time compared to the runaway avalanche time, the conversion of the plasma current into runaway current can be decreased significantly.

If the strategy of preventing the formation of a large fraction of runaway current fails, a last defense to protect the machine is to keep the runaway current away from the first wall and to dissipate it by impurity injection. The dissipation of the runaway current has been demonstrated in several devices like DIII-D, JET and J-TEXT [27–29]. The enhanced drag due to the impurities and the enhancement of the runaway electron synchrotron radiation due to pitch angle scattering when colliding with the impurity ions can have a significant effect on the dissipation of the runaway beam. Nevertheless, the suppression of runaway electrons by MGI or SPI is still an open question since the mixing impurity efficiency in the plasma is only 25% of the Rosenbluth density for complete suppression of the runaway electrons [30, 31].

The decoupling of runaway electrons by destroying magnetic surfaces can act as an auxiliary method for complete runaway suppression. The currents induced by a disruption in the first wall such as in the blanket modules has been proposed to act as fail-safe prevention of the re-formation of magnetic surfaces and prevention of runaway formation [32]. It has the benefit of preventing the conversion of plasma current into runaway current when the disruption precaution time for a disruption is not long enough for the active disruption mitigation system. The magnetic perturbation is still a prospective auxiliary method for runaway suppression.

It has been proven that the magnetic perturbation is a potential tool for the suppression of runaway electrons on JT-60U and TEXTOR [33–36]. The experimental results on TEXTOR have indicated that the argon injection induced runaway current can be suppressed by RMP with enough strength [36]. However, the RMP has not been successful in suppressing the runaway generation during disruptions for the large machine JET [37]. This is probably due to the large distance of the RMP coils to the plasma and the large plasma size. Several simulations have been performed to investigate the mechanism of runaway suppression by RMP and the possibility of runaway suppression by RMP for the next generation machine ITER [38–41]. The numerical work based on the ITER ELM configuration suggested that runaway loss can be significant enhanced in the regions where the normalized perturbation amplitude is higher than $\delta B/B \approx 10^{-3}$. In addition, the theoretical result has also demonstrated this magnetic perturbation threshold for runaway suppression [42]. With the maximum current (60 kA) in the ITER RMP coils, this perturbation level can be generated at the flux-surface $\psi = 0.45$–0.5, which would not be enough for the deep penetration required in ITER. For large-scale machines, an alternative choice is to induce mode locking by RMP in plasma with MHD activities. Mode locking can occur with the magnetic perturbation as small as $\delta B/B \approx 10^{-4}$ in ITER [43], which is much lower than the perturbation level of mode penetration. Therefore, it might be practical for a large size machine.

The effect of RMP mode locking on runaway suppression has been studied on J-TEXT for further understanding of the suppression effect. The complete suppression of runaway generation during disruptions by mode locking with the application of external magnetic perturbation has been verified on the J-TEXT tokamak. The magnetic perturbations have the advantage of decoupling the runaway seeds before they reach high energies. Robust runaway suppression has been reached on J-TEXT with mode locking by the application of resonant magnetic perturbations (RMP) with $m/n = 2/1$ before the thermal quench. The mode locking implemented large magnetic islands inside the plasma which act as explosive bombs during disruptions and lead to stronger stochasticity in the whole plasma cross section. The paper is organized as follows. The introduction of the J-TEXT tokamak is presented in section 2. The suppression of runaway generation by mode locking in fast shutdown experiments is discussed in section 3. The simulation results from NIMROD are shown in section 4. Lastly, the summary is presented in section 5.

2. Experimental setup

J-TEXT is a conventional tokamak with an iron core [44]. It has a major radius of $R = 105$ cm. The minor radius can be modified in the ranges of 25 cm–29 cm by a movable titanium-carbide coated graphite limiter. The maximum toroidal magnetic field is $B_T = 2.3$ T. The maximum plasma current is $I_p = 220$ kA with a 600 ms pulse length. The central line averaged electron density is in the range of $n_e = (1–6) \times 10^{19}$ m^{-3}.

A multichannel FIR interferometer with seven channels that cross the J-TEXT cross-section vertically has been employed to measure the electron density. There are two poloidal arrays of 2D Mirnov coils and one toroidal array mounted inside the vessel for the detection of MHD activities. Three AXUV arrays are used to measure the total radiated power and the radiation profile. The hard x-ray radiation (HXR) in the energy range of 0.5–5 MeV resulting from the thick target bremsstrahlung when runaway electrons are lost from the plasma and impinge on the vessel walls is measured by two NaI(Tl) detectors with collimators. One NaI(Tl) detector is arranged in the electron approach direction. The other one is arranged in the radial direction. In order to prevent the saturation of the detector, a lead brick with 1 cm in thickness was placed before the collimators. Thus the low energy HXR was cutoff in the measurement. A vertical soft x-ray pinhole camera located at the top of the vessel is used to measure the disruption generated runaway beam. It is used to measure the profile of soft x-ray emissions and also the sawtooth activities.

Two MGI valves have been developed for the study of the fast plasma shutdown experiments on the J-TEXT tokamak. A 30 ml MGI valve has been installed at bottom port of No. 9. It can be operated in the ranges of 5–30 bar. Another 60 ml MGI valve has been installed at top port of No. 9. It can be operated in the ranges of 5–40 bar. They are based on the eddy-current repulsion mechanism. The piston of the MGI valve is made by non-ferromagnetic material so that it can be installed as close as possible to the vacuum vessel. The valves are about 0.5 m away from the plasma boundary. A main feature of the MGI valve is that the coil is installed separately with the mushroom cap of the piston and connected with the atmosphere [45]. Thus the temperature of the coils can be kept to a low value. The pulse current is produced by a discharge circuit, which is triggered by the central control system. A high-speed camera has been used to calibrate the moving distance of the piston. It shows that the reaction time of the MGI valve is about 0.3 ms. The MGI valve can be kept open on the order of 10 ms. The maximum density of the injected impurities is more than 100 times that of the plasma inventory.

There are two sets of resonant magnetic perturbation (RMP) systems to induce the magnetic perturbations in the plasma and for the analysis of their effects on the runaway electrons [44]. The static RMP coils are located outside of vessel. The dynamic RMP coils are located inside of vessel and can be operated both in DC mode and in AC mode. They can be operated in $m/n = 2/1$ dominated mode or 3/1 dominated mode.

3. Suppression of runaway generation by mode locking

The MGI of a small amount of Ar can produce stable runaway current plateau in J-TEXT. The generation of runaway current in disruption depends on the plasma parameters. The regime of runaway generation during disruptions with different toroidal magnetic fields B_T and different edge safety factors q_a has been investigated in J-TEXT as shown in figure 1. In order to prevent the effect of plasma density on the runaway generation, the plasma density is kept at about 1×10^{19} m^{-3}, which is optimal for the generation of runaways. It is found that the runaways can be generated with much lower magnetic field $B_T = 1.4$ T when the edge safety factor q_a is large enough, $q_a > 3.5$. The threshold of q_a decreases with increasing B_T. The threshold of q_a at $B_T = 2$ T is about 2.8. With lower edge safety factor, the plasma becomes more unstable, which favors runaway free disruptions. For $q_a = 2.8$ at $B_T = 2$ T there are strong 2/1 tearing modes. A typical disruption with strong $m/n = 2/1$ mode which produced an ~120 kA runaway current plateau in shot #1044530 is shown in figure 2. In this shot, the $m/n = 2/1$ tearing mode with frequency of 5 kHz was identified from Mirnov signal. The Ar MGI was triggered at 0.4 s. The line averaged electron density increased to a higher level in 2 ms accompanied by the fast drop of the amplitude of the electron cyclotron emission (ECE) signal, which indicated the thermal quench occurred. Subsequently, the current quench occurred with a significant decay of plasma current and 150 V loop voltage was produced during this phase. A stable runaway current plateau was formed in this target.

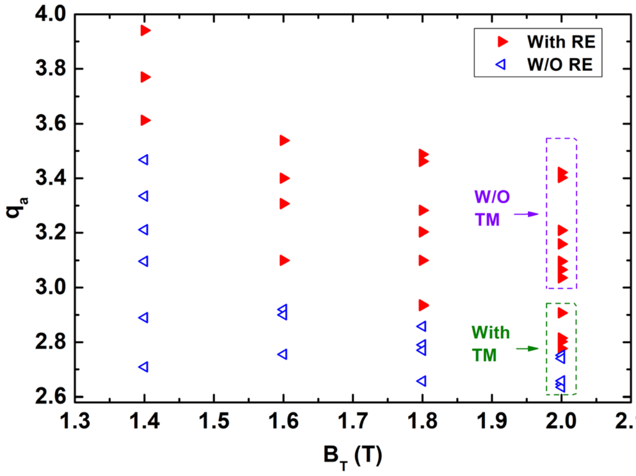

Figure 1. Regime of runaway generation during disruption for q_a versus B_T on J-TEXT. TM: tearing mode. There are strong 2/1 tearing modes for $q_a = 2.8$ at $B_T = 2$ T, which are disrupted with runaway current plateau formation.

With stronger MHD activities, it is possible to suppress the generation of runaway current during disruptions. The magnetic islands of $m/n = 2/1$ mode can be enlarged by slowing down the plasma rotation. The mode locking is an alternative to changing the size of the magnetic islands. The effect of $m/n = 2/1$ mode locking by RMP on runaway current generation during disruptions has been carried out recently. The static RMP coils with $m/n = 2/1$ configuration of the resonant magnetic perturbation fields was used to lock the preexisting magnetic islands before disruption. The 4 kA RMP with 2.8 Gs $m/n = 2/1$ B_r was applied at 0.36 s in shot #1044915, as shown in figure 3. It was found that the frequency of the $m/n = 2/1$ mode as indicated from the Mirnov signal gradually slowed

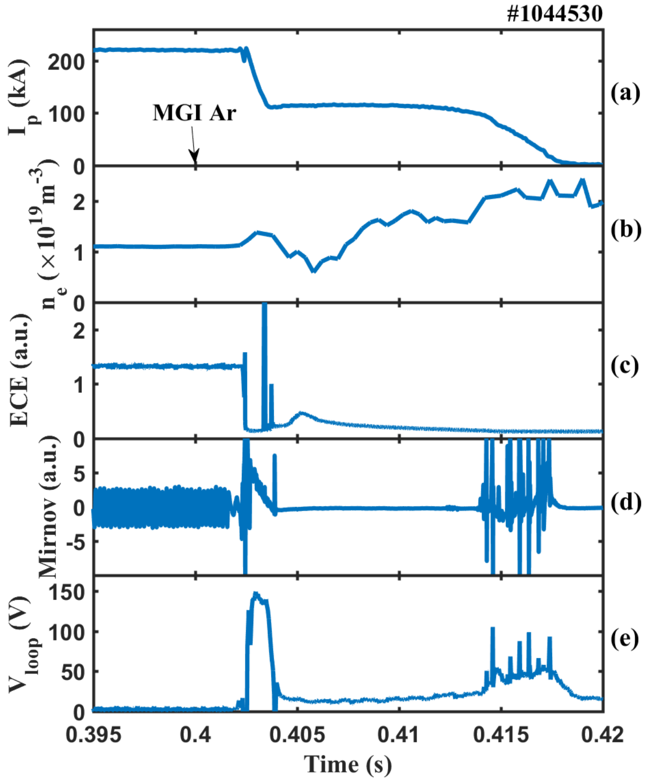

Figure 2. Temporal evolution of typical disruption with the 2/1 mode which formed a runaway current. The Ar MGI is triggered at 0.4 s. From the top to bottom, the waveforms are: (*a*) the plasma current, (*b*) the central line averaged electron density, (*c*) ECE signal at the radial position of 7.54 cm, (*d*) Mirnov signal, (*e*) the loop voltage.

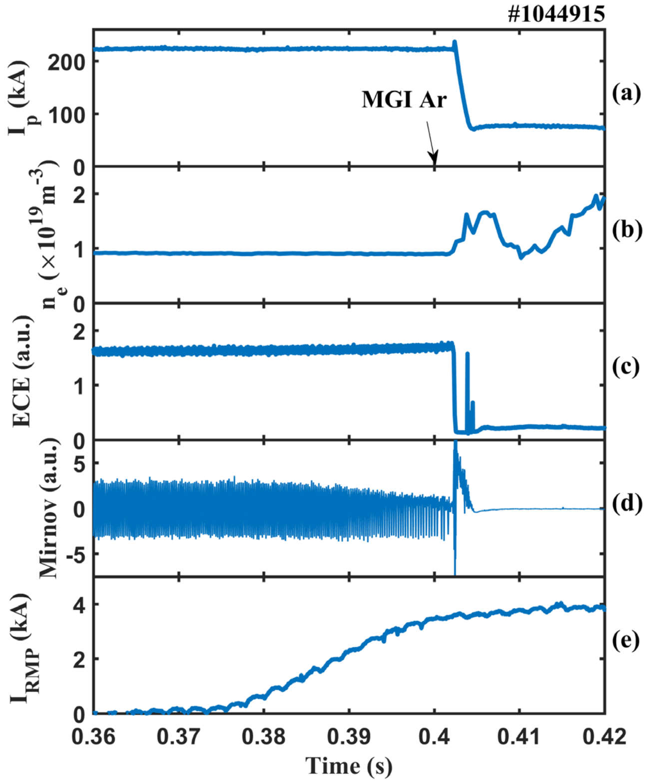

Figure 3. Temporal evolution of plasma current, central line averaged electron density, ECE signal at the radial position of 7.54 cm, Mirnov signal, and RMP current in shot #1044915 with partial mode locking. The Ar MGI is triggered at 0.4 s. The static RMP was applied at 0.36 s with 2.8 Gs for $m/n = 2/1$ mode. The runaway current was partially suppressed by the application of RMP.

down with an increase of RMP current. The MGI was fired at 0.4 s when the mode locking did not occur in the end. At about 76 kA the runaway current was produced during disruption, less than the runaway current of the reference shot #1044530, which demonstrated that the large magnetic islands have the ability to reduce the production of RE by enhancing the runaway loss rate with stronger MHD activities. In order to generate locked modes in the target plasma, the RMP was turned on at 330 ms in shot #1044918, as shown in figure 4. Similarly, the amplitude of Mirnov oscillations decreased with the increasing of the RMP current and approached zero before disruption. The mode locking happened at 0.385 s, which is 15 ms in advance of the MGI trigger time. The runaway current was completely suppressed in this shot. Comparing the two shots above, it seems that the mode locking before disruption is the key for the runaway current suppression. It is generally accepted that large magnetic islands will result in a large area of magnetic topology stochasticity during disruptions. When the MGI is fired, a large region of magnetic surface is broken up due to the large islands in the mode-locking target, which could decouple RE seeds and prevent REs from reaching relativistic energies. Ultimately, the stochastic magnetic fields spread to the core so that all of RE seeds are lost to the first wall before they reach high energy.

Considering the effect of mode locking on the runaway current, the RMP was applied at different times before the disruption was triggered. The statistics results are shown in figure 5. The time of mode locking in this figure means the time interval between the mode locking and the Ar MGI trigger time. With the same plasma parameters and an equal amount of argon injection, mode locking occurred at a different time. All shots without mode locking are marked by blue inverted triangles in the diagram. There are stable runaway current plateaus in the reference shots without mode locking. The runaway current can be completely suppressed when the mode locking happened 4 ms ahead of the MGI trigger time.

The RMP field not only affects the rotation frequency of the magnetic islands, but simultaneously also affects the size of the magnetic islands. With the increase of RMP amplitude, the rotating magnetic islands can be slowed down and the size of magnetic islands increased. The magnetic island will increase to a saturated size if the mode locking is occuring at least 4 ms before the MGI trigger time. A small increase in the size of the magnetic island when the mode locking is 2.5 ms in advance of the MGI trigger results in the survival of runaway current as shown in figure 5. The loss rate of runaway electrons during disruption is dominated by the stochasticity of the magnetic field, which depends on the size of the magnetic islands in the pre-disruption plasma. The large magnetic islands inside the plasma act as an explosive bomb and lead to stronger stochasticity in the whole plasma cross section during disruptions, which could enhance the loss of runaway electron seeds and suppress the generation of runaway current.

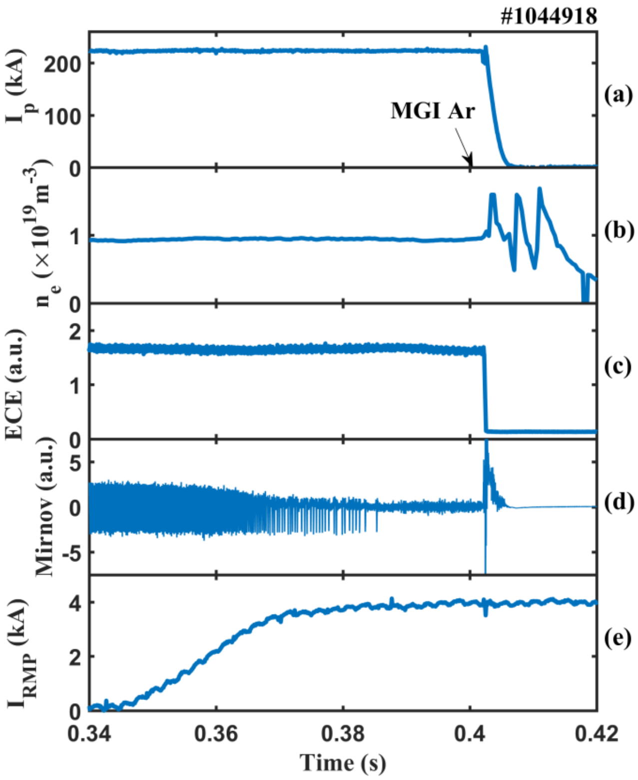

Figure 4. Temporal evolution of plasma current, central line averaged electron density, ECE signal, Mirnov signal, and RMP current in shot #1044915 with mode locking. An Ar MGI is triggered at 0.4 s. The static RMP was applied at 0.33 s with 2.8 Gs for $m/n = 2/1$ mode. The runaway current was completely suppressed by the mode locking occurring at 0.385 s.

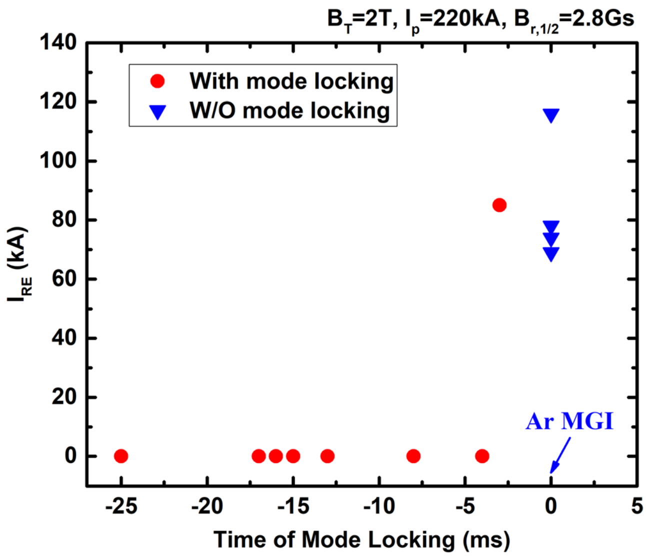

Figure 5. Dependence of the runaway current on the time of mode locking before the disruptions. All shots without locked mode are marked by blue inverted triangles at $t = 0$ s. The red solid circles correspond to time of occurrence of mode locking. The runaway current can be robustly suppressed by mode locking, if occurs 4 ms ahead of the MGI trigger time.

4. NIMROD simulation of runaway suppression

The NIMROD (non-ideal MHD with rotation, open discussion) extended MHD code [46–49] was used to simulate the plasma response to an externally applied resonant magnetic perturbation on the J-TEXT tokamak [50]. For J-TEXT, the experimental Lundquist numbers fall in the range of 10^6–10^7, and in order to reduce the expense of the computation, the real Lundquist number used is 10^5 by enhancing the resistivity artificially in this simulation. The plasma equilibrium parameters, such as plasma current density, pressure and magnetic field, were obtained from EFIT. The two thermal transport coefficients are $\chi_\perp = 1$ m^2 s^{-1} and $\chi_\parallel = 10^8$ m^2 s^{-1}. The initial pitch angle is 0.1 rad and is uniform along the radial direction. When an error field is applied, the mode locking occurs after 0.2 ms. The magnetic topology with $m/n = 2/1$ islands has been used to simulate the confinement of REs in order to study the effect of mode locking on the confinement of runaway seeds as shown in figure 6(*a*). The disruption is triggered by the deposition of a large amount of Ar in the simulation. During the pre-TQ and the subsequent TQ stage, a series of MHD activities were induced. The drift-orbit losses for the test population of REs were calculated to determine the confinement time of the RE population. At the beginning of calculation, 1900 REs with 5 MeV kinetic energy were distributed randomly on the area of a poloidal cross section at a certain toroidal angle. When the Ar gas reached the plasma, the current channel was contracted and the locked islands resulted a large regime of stochasticity following disruption as shown in figure 6(*b*). For the REs with 5 MeV initial kinetic energy, when MGI was turned on, after 0.2 ms evolution, the fraction of REs lost was up to 50% during the stochastic phase with mode locking as shown in figure 7(*a*). But for the disruption target without mode locking, only 10% fraction of REs were lost in the simulation in the first 0.2 ms stage of the disruption, which is much lower than the mode locking case. And, as shown in figure 7(*b*), the same conclusion can be obtained for the REs with 50 keV initial kinetic energy, but the REs escape time is obviously increased for the case without mode locking. This result indicates that the mode locking is very beneficial to the mitigation of seed REs.

For the mode locking case, the stochasticity of the magnetic surfaces during disruption occurred much faster than that without mode locking, thus the REs were easier to transport to the outside of plasma. The high fraction of REs lost in mode locking resulted in the runaway current suppression, which was consistent with the experiment result. Thus it suggested that mode locking could effectively suppress the runaway current due to the large magnetic islands resulting in a larger regime of stochasticity at the beginning of the disruption which expelled the runaway seeds.

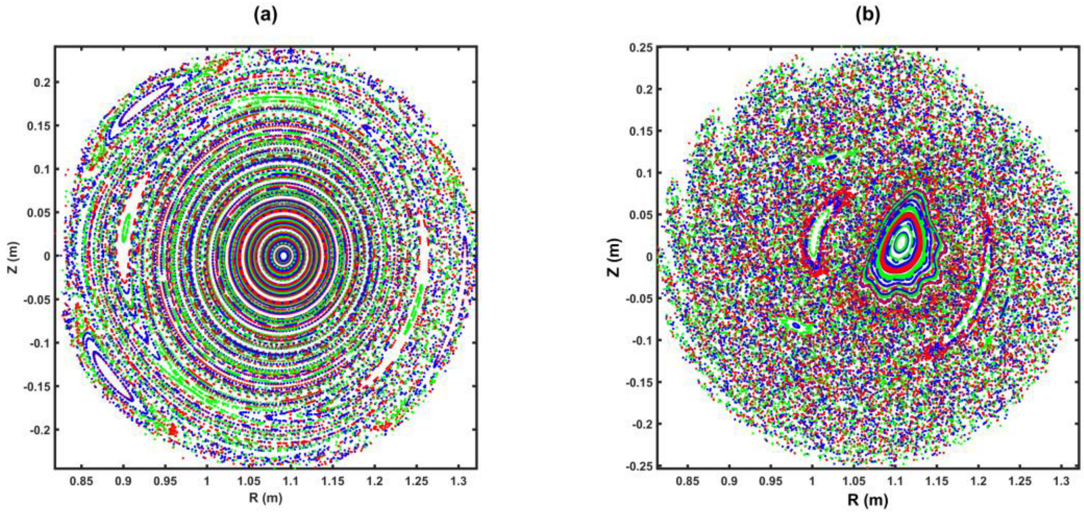

Figure 6. Evolution of magnetic fields presented by magnetic Poincare plot with a mode-locking target. (*a*) Magnetic Poincare plot with magnetic islands by RMP mode locking 0.2 ms after MGI injection, (*b*) Magnetic Poincare plot with strong stochasticity in the plasma cross section after 3 ms.

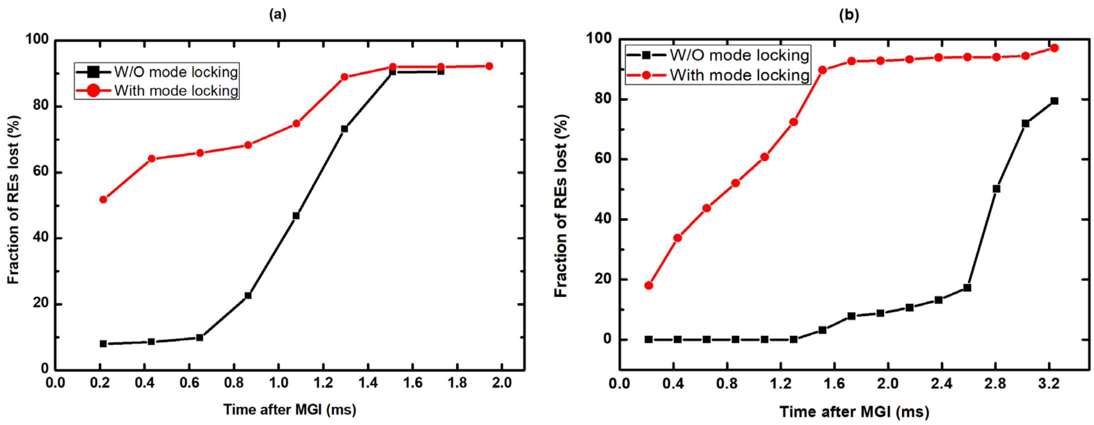

Figure 7. Comparison of the fractions of runaway electrons lost with mode locking and without mode locking during disruptions by NIMROD simulation. (*a*) The initial REs with 5 MeV kinetic energy. At the beginning of current quench, the fraction of REs lost is up to 50% in the mode locking case which is much higher than that without mode locking. (*b*) The initial REs with 50 keV kinetic energy. The fraction of REs lost is about 20% at the beginning of current quench with mode locking which is higher than that without mode locking.

5. Summary

In summary, the effect of mode locking on the suppression of runaway current during disruptions has been investigated on J-TEXT. The static RMP was used to slow down the rotation of magnetic islands preexisting in target plasma and generated mode locking before disruption. It was found that the runaway current could be robustly suppressed by mode locking which occurred 4 ms ahead of an MGI triggered disruption. With partial mode locking, the runaway current could be partially suppressed which indicated the large magnetic islands have the ability to reduce the production of RE seeds. Since the transport of runaway electrons is dominated by the magnetic fluctuations, the larger magnetic islands existing in the pre-disruption plasmas could enhance the stochastic regime, which resulted in rapid loss of RE seeds during disruption. A NIMROD simulation has been performed to study the transport of runaway electrons during disruptions on J-TEXT. For the mode locking case, a larger regime of magnetic topology stochasticity was formed than the case without mode locking due to the pre-existing large magnetic islands. The fraction of REs lost is up to 50% at the beginning of disruption with mode locking which is much higher than that without mode locking for the 5MeV initial kinetic energy REs. It indicates that the mode locking leads to strong stochasticity in the whole plasma cross-section and expels the runaway seeds. This simulation result suggested that the mode locking in pre-existing magnetic island plasma can effectively suppress the runaway electrons during disruptions. Thus, the application of RMP to generate mode locking in target plasmas with strong MHD activities is an alternative to mitigate runaway electrons in tokamak plasmas.

Acknowledgments

The authors are very grateful to help with J-TEXT team. This work was partially supported by the National Natural Science Foundation of China (Nos. 11775089, 71762031 and

11575068) and by the National Magnetic Confinement Fusion Science Program (Nos. 2015GB111002, 2015GB104002 and 2015GB104004). Simultaneously, the authors thank Dr A.C. England for technical discussions and Dr Izzo for her kindly help about NIMROD.

References

[1] Riccardo V. and JET EFDA Contributors 2003 *Plasma Phys. Control. Fusion* **45** A269
[2] Sebiiller F.C. 1995 *Plasma Phys. Control. Fusion* **37** A135
[3] Hender T.C. *et al* 2007 *Nucl. Fusion* **47** S128
[4] Pautasso G. *et al* 2007 *Nucl. Fusion* **47** 900
[5] Putvinski S. *et al* 1997 *Plasma Phys. Control. Fusion* **39** B157
[6] Commaux N. *et al* 2010 *Nucl. Fusion* **50** 112001
[7] Jaspers R. *et al* 1993 *Nucl. Fusion* **33** 1775
[8] Smith H.M. and Verwichte E. 2008 *Phys. Plasmas* **15** 072502
[9] Bozhenkov S.A. *et al* 2008 *Plasma Phys. Control. Fusion* **50** 105007
[10] Russo A.J. and Campbell R. B. 1993 *Nucl. Fusion* **33** 1305
[11] Gill R.D. *et al* 2000 *Nucl.Fusion* **40** 163
[12] Jaspers R. *et al* 1996 *Nucl. Fusion* **36** 367
[13] Plyusnin V.V. *et al* 2006 *Nucl. Fusion* **46** 277
[14] Gál K. *et al* 2008 *Plasma Phys. Control. Fusion* **50** 055006
[15] Pautasso G. *et al* 1996 *Nucl. Fusion* **36** 1291
[16] Yoshino R. *et al* 1997 *Plasma Phys. Control. Fusion* **39** 313
[17] Taylor P.L. *et al* 1999 *Phys. Plasmas* **6** 1872
[18] Zeng L. *et al* 2013 *Phys. Rev. Lett.* **110** 235003
[19] Wongrach K. *et al* 2014 *Nucl. Fusion* **54** 043011
[20] Wongrach K. *et al* 2015 *Nucl. Fusion* **55** 053008
[21] Abdulaev S.S. *et al* 2015 *Phys. Plasmas* **22** 040704
[22] Granetz R.S. *et al* 2014 *Phys. Plasmas* **21** 072506
[23] Martin-Solis J.R. *et al* 2014 *Nucl. Fusion* **54** 083027
[24] Lehnen M. *et al* 2009 *J. Nucl. Mater.* **390–1** 740
[25] Reux C. *et al* 2010 *Nucl. Fusion* **50** 095006
[26] Chen Z.Y. *et al* 2013 *Plasma Phys. Control. Fusion* **55** 035007
[27] Yoshino R. *et al* 1999 *Nucl. Fusion* **39** 151
[28] Hollmann E.M. *et al* 2013 *Nucl. Fusion* **53** 083004
[29] Reux C. *et al* 2015 *Nucl. Fusion* **55** 129501
[30] Hollmann E.M. *et al* 2015 *Phys. Plasmas* **22** 021802
[31] Lehnen M. *et al* 2015 *J. Nucl. Mater.* **463** 39
[32] Boozer A.H. 2011 *Plasma Phys. Control. Fusion* **53** 084002
[33] Yoshino R. and Tokuda S. 2000 *Nucl. Fusion* **40** 1293
[34] Finken K. *et al* 2007 *Nucl. Fusion* **47** 91
[35] Finken K. *et al* 2006 *Nucl. Fusion* **46** S139
[36] Lehnen M. *et al* 2008 *Phys. Rev. Lett.* **100** 255003
[37] Riccardo V. *et al* 2010 *Plasma Phys. Control. Fusion* **52** 124018
[38] Papp G. *et al* 2011 *Nucl. Fusion* **51** 043004
[39] Papp G. *et al* 2011 *Plasma Phys. Control. Fusion* **53** 095004
[40] Papp G. *et al* 2012 *Plasma Phys. Control. Fusion* **54** 125008
[41] Matsuyama A. *et al* 2014 *Nucl. Fusion* **54** 123007
[42] Feher T. *et al* 2011 *Plasma Phys. Control. Fusion* **53** 035014
[43] Buttery R. J. *et al* 1999 *Nucl. Fusion* **39** 1827
[44] Zhuang G. *et al* 2013 *Nucl. Fusion* **53** 104014
[45] Luo Y.H. *et al* 2014 *Rev. Sci. Instrum.* **85** 083504
[46] Sovinec C.R. *et al* 2004 *J. Comput. Phys.* **195** 355
[47] Izzo V.A. *et al* 2011 *Nucl. Fusion* **51** 063032
[48] Izzo V.A. *et al* 2012 *Plasma Phys. Control. Fusion* **54** 095002
[49] Izzo V.A. *et al* 2017 *Phys. Plasmas* **24** 060705
[50] Li B.C. *et al* 2017 Numerical simulation of plasma response to the externally applied resonant magnetic perturbation on J-TEXT *Plasma Sci. Technol.* accepted